Research Article

Peng Li, Jiajun Yu, Shaohua Jiang*, Hong Fang, Kunming Liu, and Haoqing Hou*

Dielectric, mechanical and thermal properties of all-organic PI/PSF composite films by *in situ* polymerization

https://doi.org/10.1515/epoly-2020-0020
received February 15, 2020; accepted March 20, 2020

Abstract: All-organic high dielectric materials are highly required in the field of modern electronic industry and energy storage. In this work, all-organic polyimide/polysulfone composite films with different amounts of PSF (PI/PSF-*X*) were prepared by *in situ* polymerization followed by film casting and thermal treatment. The dielectric, mechanical and thermal properties of these PI/PSF-*X* composite films are characterized by dielectric measurement, tensile test, thermogravimetric analysis and dynamic mechanical analysis. The results suggest that the PI/PSF-*X* composite films have good dielectric properties, good mechanical properties and excellent thermal properties, which are suitable for applications in electronic devices in harsh environments, especially in high-temperature environments.

Keywords: polysulfone, polyimide, dielectric properties, mechanical properties, thermal properties

1 Introduction

With the development of modern electronics, polymer-based all-organic dielectric composites are highly required because of their excellent mechanical flexibility, light weight, easy fabrication process, and their dielectric properties (1–3). There are many reports regarding polymer-based all-organic composites with a high dielectric constant, such as polypyrrole/poly(vinylidene fluoride–chlorotrifluoroethylene) (PPy/PVDF-CTFE) (4), PANI–DBSA/PVDF (5), PVDF/(PCMS-*g*-CuPc) (6), PPy/P(VDF-TrFE) (7) and DIPAB/PVDF (8). Although these composite systems present good dielectric performance, their mechanical properties and thermal stability are inevitably decreased because of the addition of organic fillers. Therefore, it is still highly desired to search for good polymer-based all-organic systems for the application of high dielectric materials.

It is well known that polyimides (PIs) are high-performance polymers with excellent thermal stability, mechanical property and high dielectric breakdown strength (9–14). However, PIs are not the ideal high dielectric materials because of their low permittivity in the range of 2.5–3.5, which greatly limits their applications in electronic products (15–20). In general, there are three strategies to improve the dielectric properties of PIs. One is to introduce functional groups into the main chains of PIs by molecular design. Peng et al. obtained a PI with a dielectric constant of 7.1 by introducing bipyrimidine units into the main chains of PI, and the complex formed by this PI and copper has a dielectric constant up to 133 (21). Yang et al. synthesized a PI containing crown ether groups in the main chain to increase the polarization of the molecular chains, and this PI has a dielectric constant of 5.4–6.9 and a dielectric loss less than 0.03 in the frequency range of 100 Hz to 100 kHz (22). However, this method often involves very complex synthesis procedure. At the same time, the introduction of functional groups will reduce the reactivity of monomers, resulting in low yield and low molecular weight (23). Another strategy is to add high dielectric inorganic fillers or conductive particles to fabricate high dielectric PI composite materials (24–26). Xie et al. used 50 vol% barium titanate to raise the permittivity of PI to 35 (27). Xu et al. prepared PI/multi-walled carbon nanotubes (MWCNT)

* **Corresponding author: Shaohua Jiang,** Co-Innovation Center of Efficient Processing and Utilization of Forest Resources, College of Materials Science and Engineering, Nanjing Forestry University, Nanjing 210037, China, e-mail: shaohua.jiang@njfu.edu.cn
* **Corresponding author: Haoqing Hou,** College of Chemistry and Chemical Engineering, Jiangxi Normal University, Nanchang 330022, China; Jiangxi Nanofiber Engineering Technology Research Center, Nanchang 330022, China, e-mail: haoqing@jxnu.edu.cn
Peng Li, Jiajun Yu: College of Chemistry and Chemical Engineering, Jiangxi Normal University, Nanchang 330022, China; Jiangxi Nanofiber Engineering Technology Research Center, Nanchang 330022, China
Hong Fang: College of Chemistry and Chemical Engineering, Jiangxi Normal University, Nanchang 330022, China
Kunming Liu: School of Metallurgical and Chemical Engineering, Jiangxi University of Science and Technology, Ganzhou 341000, China

nanocomposites by electrospinning, with a dielectric constant of up to 147–161 (at 1 kHz) (28). This strategy can not only greatly improve the dielectric constant but also bring three disadvantages. First, in this method, it is usually difficult to disperse fillers uniformly in the PI matrix. Second, with this strategy, the dielectric loss is relatively high, which would lead to an increased temperature and further influence the safety of electronic devices. Third, the flexibility of composites would be rapidly reduced because of filler agglomeration and phase separation.

Therefore, it would be a good choice to incorporate organic fillers to solve the aforementioned issues. For example, Zhang et al. added β-cyclodextrin to toughen and improve the dielectric properties of PIs (24). In another report, Shen et al. enhanced PVDF with PI nanofibers and obtained a composite film with good dielectric properties and mechanical properties (17). However, the thermal stability and mechanical properties of these organic fillers are not better than those of PIs. Therefore, the thermal performance and mechanical properties of these composites do not exhibit good performance, which greatly limits their practical applications. So, it is still highly required to search for good organic fillers for the modification of PI.

It is well known that polysulfone (PSF) is also a high-performance polymer with a relatively high dielectric constant as well as good mechanical flexibility (29–31). However, its thermal stability, electrical breakdown strength and mechanical properties are lower than those of PI. In this work, we choose PI and PSF to produce composite films by an *in situ* polymerization. On one hand, the precursor of both PSF and PI, polyamic acid (PAA), could be dissolved in polar solvents, such as *N*,*N*′-dimethylacetamide (DMAc) and *N*,*N*′-dimethylformamide (DMF), leading to a good compatibility in the molecular level. On the other hand, the properties of PI and PSF could complement each other's advantages, therefore achieving the goal of high dielectric polymer composite films for further applications in electronic devices.

2 Experimental

2.1 Materials

PSF (Tanlon®fiber T500) was provided by Shanghai Tanlon Fiber Co., Ltd, China. It was boiled in absolute ethanol and then dried before use. DMAc (≥99%; Sigma-Aldrich) was dried and distilled before being used. 3,3′,4,4′-Biphenyltetracarboxylic dianhydride (BPDA) and 4,4′-oxydianiline (ODA) were purchased from Hebei Jida Plastic Products Co., China, and purified by sublimation before use.

2.2 Preparation of PI/PSF-*X* composite films

PSF solution at a concentration of 10 wt% was prepared by dissolving PSF in DMAc. Then ODA and BPDA in an equal molar ratio were added into the PSF solution. The mixture was vigorously stirred at −5°C for 12 h to obtain a PAA/PSF mixture. The amount of PSF in the mixture was set to 0, 5, 10, 15, 20, 25, 30, 40 and 100 wt% by controlling the amount of BPDA and ODA. Then the PAA/PSF solution was coated on a clean glass plate (8 mm × 8 mm) and dried at 60°C for 24 h. Finally, the PAA/PSF composite films were thermally treated in a high temperature furnace in N_2 to convert the PAA to PI. The heating procedure is as follows: (1) heating to 150°C (2°C/min) and maintaining for 60 min to remove the residual solvent and for partial imidization of PAA to PI; (2) heating to 350°C (2°C/min) and maintaining for 120 min to imidize completely to form PI; and (3) cooling to the room temperature. The resultant PAA/PI and PSF/PI composite films are represented as PAA/PSF-*X* and PI/PSF-*X*, respectively, where *X* stands for the initial ratio of PSF in the composites.

2.3 Characterization

Thermogravimetric analysis (TGA) was measured by WRT-3P (Shanghai) at a heating rate of 10°C/min under N_2. Dynamic mechanical analysis (DMA) in tension mode was performed on a PerkinElmer Pyris diamond analyzer under the conditions of a heating rate of 3°C/min, a frequency of 1 Hz and an amplitude of 5 μm in N_2. The mechanical properties of composite films were measured using an electromechanical universal testing machine (CMT 8102; SANS, Shenzhen, China) at a stretching speed of 5 mm/min. The dielectric permittivity of composite films was measured using a precision LCR meter (TH2819A; Tonghui, Changzhou, China) with a sample size of about 8 × 8 mm and a thickness of 20–40 μm, wherein conductive adhesive covered on the two sides served as the electrodes, and the thickness was measured using a screw meter. The dielectric breakdown strength of the films was measured using an electric breakdown strength test machine (KP8048, Dongguan, China) in air and at room temperature.

3 Results and discussion

3.1 Fabrication of PI/PSF-*X* composite films

The preparation process of PI/PSF-*X* composite films is shown in Figure 1. PSF has a good solubility in the solvent of DMAc. After adding the monomers ODA and BPDA into the PSF solutions, *in situ* polymerization occurred and finally gave rise to PAA/PSF solution. After casting and thermal treatment, PI/PSF-*X* composite films were obtained. As shown in Figure 1, the PAA/PSF solution is very clear, suggesting the homogeneous mixing of PAA and PSF in DMAc. The PAA/PSF and PI/PSF composite films are smooth and transparent, indicating the compatibility between PAA/PSF and PI/PSF. Further investigation on the compatibility of PI and PSF was performed by DMA, as discussed in Section 3.5.

3.2 FT-IR analysis

The chemical structures of PAA, PSF, PAA/PSF-20, PI and PI/PSF-20 composite films were characterized by Fourier-transform infrared (FT-IR) spectra (Figure 2). Comparing the FT-IR spectra of neat PAA, PI and PI/PSF-20 films, the absorption at 1,709 cm^{-1} and 1,659 cm^{-1} disappeared while two new absorption peaks at 1,778 cm^{-1} and 1,715 cm^{-1} appeared, indicating that PAA was completely converted to PI (32). In addition, the characteristic absorption peak of $-SO_2$ at 1,158 cm^{-1} in PSF (33) can be observed in PAA/PSF-20 and PI/PSF-20. Therefore, the characteristic peaks of both PSF and PI can be observed from the FT-IR spectra of PI/PSF-20, suggesting that the high temperature imidization did not influence the molecular structure of PSF.

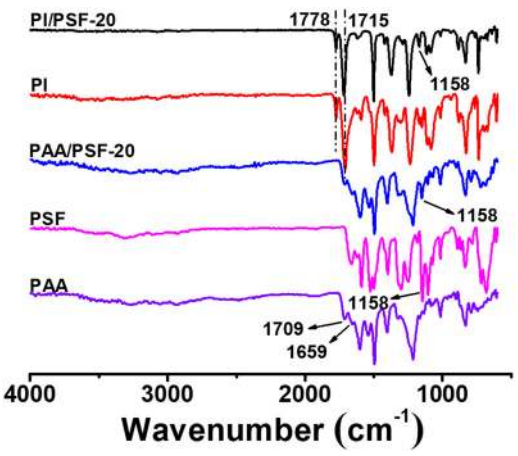

Figure 2: FT-IR spectra of pure PAA, PSF, PAA/PSF-20 and PI/PSF-20 films.

3.3 Dielectric properties

The dielectric properties of pure PI, pure PSF and their composites are shown in Figure 3 and summarized in Table 1. Figure 3a shows the frequency-dependent dielectric permittivity of the composite films. In the frequency range of 100 to 1,00,000 Hz, the dielectric constant of pure PI is slightly dependent on the frequency with values in the range of 2.75–3.25. As comparison, the dielectric constant of pure PSF is frequency dependent, with the dielectric constant decreasing from 8.92 to 7.17. When the amount of PSF was increased, the dielectric constant of PI/PSF-*X* gradually increased and the effect of frequency on the dielectric constant is not obvious. When the amount of PSF was 40 wt%, the dielectric constants of PI/PSF-40 are 6.58@100 Hz, 6.40@1,000 Hz, 6.16@10,000 Hz and 5.46@80,000 Hz, which are 2.04, 1.96, 1.99 and 1.97 times higher than those of pure PI. When the frequency is

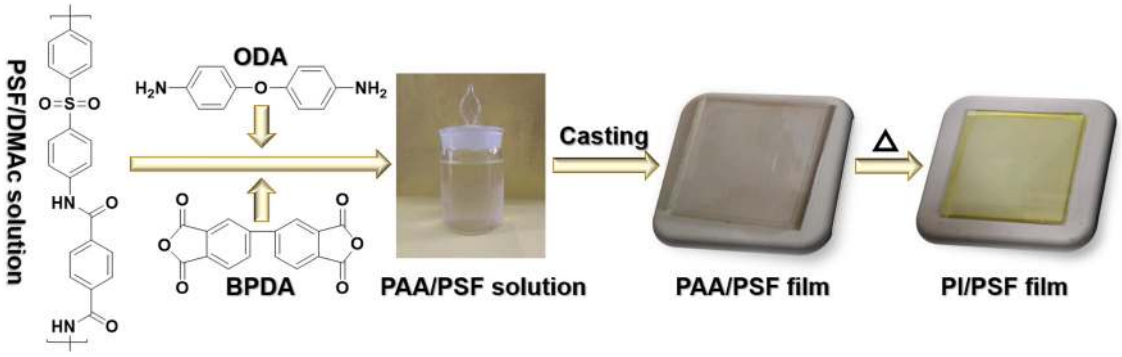

Figure 1: Schematic on the preparation of PI/PSF-*X* from PSF solutions, BPDA and ODA by *in situ* polymerization.

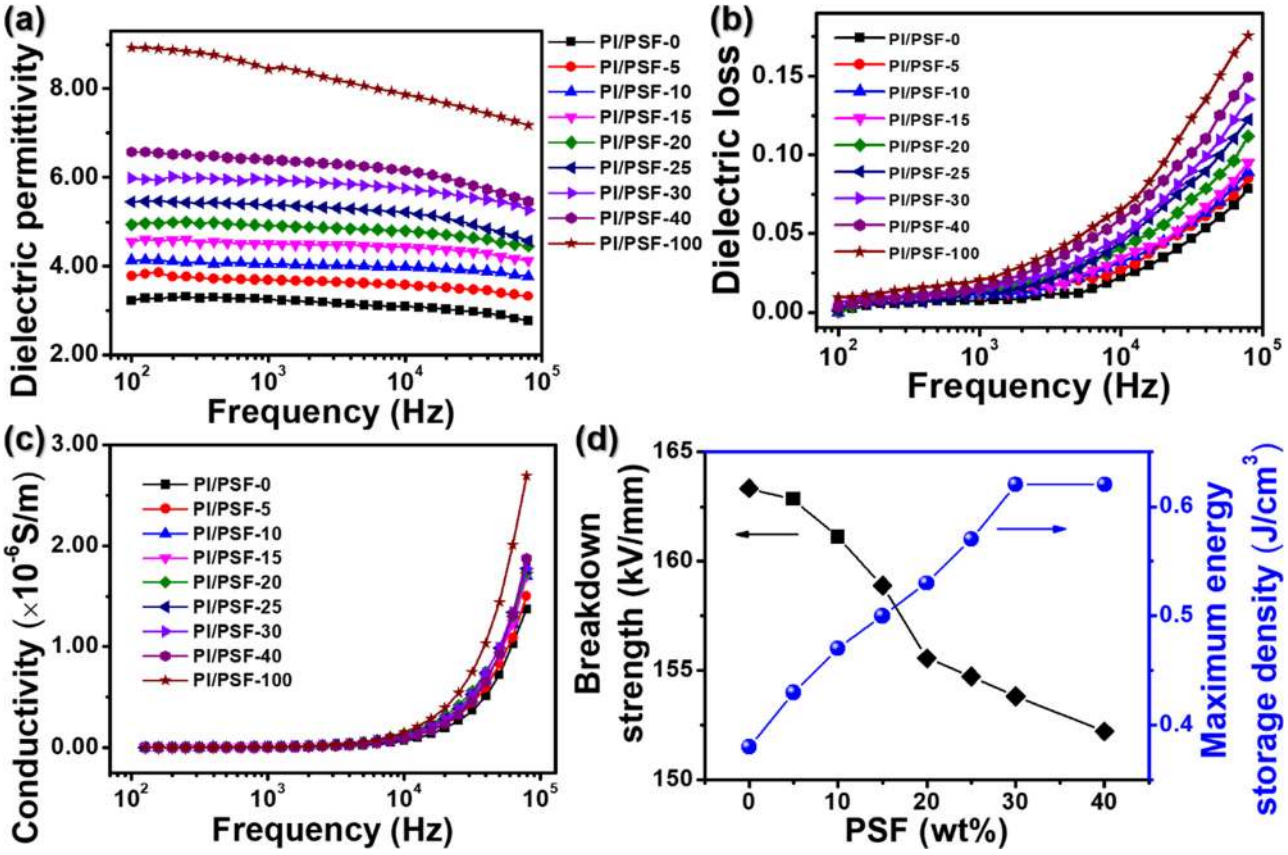

Figure 3: Frequency-dependent dielectric permittivity (a), dielectric loss (b), electrical conductivity (c) and the dielectric breakdown strength and maximum energy storage (d) of the PI/PSF-*X* composite films.

1,000 Hz, the dielectric constants of PI/PSF-5, PI/PSF-10, PI/PSF-15, PI/PSF-20, PI/PSF-25, PI/PSF-30 and PI/PSF-40 increased from 3.26, 3.69, 4.05, 4.51, 4.92, 5.38, 5.95, to 6.40, respectively. Figure 3b shows the dielectric loss of pure PI, PSF and their composites in the frequency range of 100–80,000 Hz. In general, the dielectric loss increased as the frequency increased and with the addition of PSF into the composites. When the frequency is below 1,000 Hz, the dielectric loss of all the samples is very small with values smaller than 0.02. As the frequency increased to 80,000 Hz, the dielectric loss increased up to 0.18 for the pure PSF. At the same frequency of 10,000 Hz, the dielectric loss of samples PI/PSF-5, PI/PSF-10, PI/PSF-15, PI/PSF-20, PI/PSF-25, PI/PSF-30 and PI/PSF-40 increased from 0.027 to 0.032, 0.034, 0.041, 0.044, 0.047 and 0.059, respectively. Figure 3c presents the frequency-dependent electrical conductivity of PI/PSF-*X* composite films. In general, all the samples have a very low conductivity, with values smaller than 2.69×10^{-6} s/m. The conductivity is nearly independent when the frequency is below 10,000 Hz, and gradually increased as the frequency increased from 10,000 to 80,000 Hz. The addition of PSF slightly increased the conductivity from 1.38×10^{-6} s/m (PI/PSF-0) to 1.87×10^{-6} s/m (PI/PSF-40). Such a small conductivity favors the improvement of breakdown strength and maximum energy storage density.

Compared with PSF, pure PI possesses a relatively higher breakdown strength (E_b) and a smaller maximum energy storage density (U_m). In this work, E_b of PI is 163.3 kV/mm (Figure 3d and Table 1). The addition of PSF led to a slight decrease, but still in a high level in the range of 152–163 kV/mm, which is much larger than those of other dielectric composites, such as PI/$BaTiO_3$ composite (60 kV/mm) (34), P(VDF-TrFECFE)-*g*-CuPc/PANI (<65 MV/m) (35) and PI/MWCNTs composite films (20–160 MV/m) (28). Generally, U_m can be calculated from equation (1) (24):

$$U_m = \frac{1}{2}\varepsilon_0\varepsilon_r E_b^2, \quad (1)$$

where ε_0 and ε_r are the vacuum dielectric constant (8.854×10^{-12} F/m) and relative dielectric constant, respectively. Although E_b decreases, U_m of PI/PSF composites increases due to the increase in dielectric constant (Figure 3d and Table 1). The highest U_m 0.64 J/cm^3 is achieved from sample PI/PSF-40, 68% higher than that of

Table 1: Summary of dielectric properties of PI/PSF-*X* composite films at 1,000 and 10,000 Hz

Samples	Dielectric constant		Dielectric loss		Electrical conductivity ($\times10^{-6}$ s/		E_b (kV/mm)	U_m (J/cm^3)
	1,000 Hz	10,000 Hz	1,000 Hz	10,000 Hz	1,000 Hz	10,000 Hz		
PI/PSF-0	3.25	3.09	0.0074	0.0222	0.0014	0.0714	163.3	0.38
PI/PSF-5	3.69	3.57	0.0111	0.0271	0.0050	0.0881	162.8	0.43
PI/PSF-10	4.05	3.98	0.0113	0.0318	0.0060	0.0984	161.1	0.47
PI/PSF-15	4.50	4.43	0.0129	0.0343	0.0065	0.1020	158.9	0.50
PI/PSF-20	4.91	4.79	0.0133	0.0411	0.0069	0.1031	155.6	0.53
PI/PSF-25	5.38	5.21	0.0139	0.0444	0.0071	0.1158	154.7	0.57
PI/PSF-30	5.94	5.75	0.0141	0.0474	0.0075	0.1208	153.8	0.62
PI/PSF-40	6.40	6.16	0.0155	0.0594	0.0080	0.1278	152.2	0.64
PI/PSF-100	8.44	7.87	0.0205	0.0651	0.0082	0.1484	—	—

pure PI (0.38 J/cm^3), and 256% higher than that of P(VDF-TrFECTFE/PANI) dielectric composites (0.18 J/cm^3) (36).

3.4 Mechanical properties

In electronic equipment, the mechanical properties of dielectric materials play an important role for the practical applications. Figure 4 presents the typical stress–strain curves of PSF/PI composite films, and the corresponding values are summarized in Table 2. Pure PI exhibits a tensile strength, modulus and elongation at break of 132 MPa, 3.93 GPa and 5.4%, while pure PSF possesses a lower strength of 61 MPa, a smaller modulus of 1.54 GPa, but a much higher elongation of 24.5%, respectively. When the PI and PSF were fabricated into composites, the mechanical properties of PI/PSF-*X* composites lie between those of pure PI and PSF. When the amount of PSF is 40%, the tensile strength is 93 MPa, still higher than those of other dielectric materials such as PVDF (17) and PI/$BaTiO_3$ (37). In addition, because of the good toughness of pure PSF, the elongation at break of composite films is around 10%, which is 90% higher than that of pure PI.

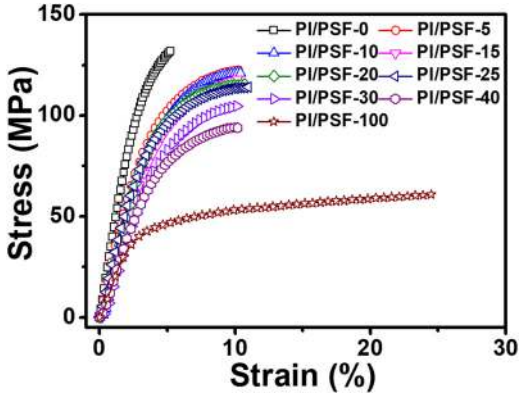

Figure 4: Mechanical properties of PI/PSF-*X* composite films.

3.5 Thermal properties

PSF possesses good thermal properties while PI has better thermal stabilities, as shown in Figure 5. Table 2 summarizes the thermal properties of PI/PSF-*X* composite films. The neat PI showed a $T_{5\%}$ and $T_{10\%}$ of 558°C and 574°C, respectively. Although PSF exhibited $T_{5\%}$ and $T_{10\%}$ of only

Table 2: Summary of mechanical and thermal properties of PI/PSF-*X* composite films

Samples	Strength (MPa)	Modulus (GPa)	Strain (%)	$T_{5\%}$ (°C)	$T_{10\%}$ (°C)	T_g (°C)
PI/PSF-0	132 ± 13	3.93 ± 0.01	5.4 ± 0.3	558	574	322
PI/PSF-5	122 ± 14	2.53 ± 0.04	10.5 ± 0.9	550	568	321
PI/PSF-10	121 ± 10	2.49 ± 0.05	10.5 ± 1.0	537	561	315
PI/PSF-15	118 ± 11	2.33 ± 0.14	10.3 ± 1.2	505	553	313
PI/PSF-20	115 ± 11	2.27 ± 0.27	10.9 ± 0.8	488	537	303
PI/PSF-25	114 ± 13	2.20 ± 0.05	11.1 ± 1.2	479	524	300
PI/PSF-30	105 ± 10	1.93 ± 0.05	10.4 ± 0.9	467	505	296
PI/PSF-40	94 ± 12	1.67 ± 0.04	10.2 ± 1.1	463	486	285
PI/PSF-100	61 ± 7	1.54 ± 0.02	24.5 ± 2.7	445	456	—

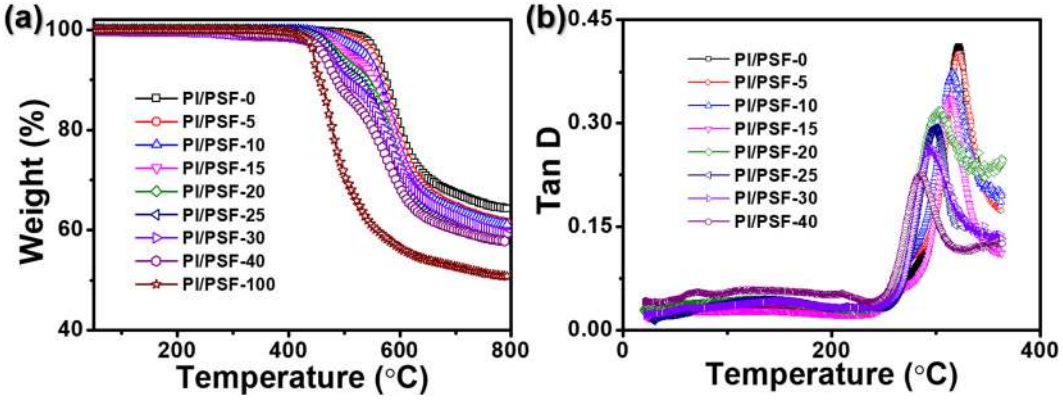

Figure 5: TGA (a) and DMA (b) curves of PI/PSF-*X* composite films.

445°C and 456°C, all the composite films still possessed $T_{5\%}$ and $T_{10\%}$ more than 463°C and 486°C, respectively. This is due to the excellent performance of the PI content. DMA is often used to characterize the glass transition temperature (T_g) of high-performance polymers with high T_g. As shown in Figure 5b and Table 2, the neat PI has one peak at around 322°C, which gradually decreased after the incorporation of PSF. Even after adding 40 wt% of PSF, T_g of the composite film remained above 280°C. These high T_g could be attributed to the slipping of PSF molecular chains during heating, which provides space for the movement of PI molecular chain. It is also worth noting that only one peak appears in the composite films in DMA, which indicates that PSF has a very good compatibility with PI because of the *in situ* polymerization of the PI precursor, PAA in PSF, and their good solubility in DMAc. TGA and DMA curves show that the PSF/PI composite films have excellent thermal performance and are expected to be applied to electronic equipment in high-temperature environments.

4 Conclusions

In summary, PI/PSF-*X* composite films with varying PSF contents have been successfully prepared by *in situ* polymerization and thermal imidization. Because they complement of each other's advantages, the PI/PSF-*X* composite films possess good dielectric performance and excellent mechanical and thermal properties. When the PSF content is 40 wt%, the PI/PSF-40 has the highest dielectric constant of 6.40@1,000 Hz, low dielectric loss of 0.0155@1,000 Hz, high E_b of 152.2 kV/mm and highest U_m of 0.64 J/cm^3. In addition, the PI/PSF-40 composite film still has excellent mechanical properties with a tensile strength of 94 MPa, elongation at break of 10.2%, $T_{5\%}$ of 463°C, $T_{10\%}$ of 486°C and T_g of 285°C. Such PI/PSF-*X* composite films with comprehensive good dielectric, mechanical and thermal properties could be good candidates for application in electronic products in complex and harsh environments, like high temperature.

Acknowledgments: This research was funded by the National Natural Science Foundation of China (21574060, 21774053 and 51903123), Major Special Projects of Jiangxi Provincial Department of Science and Technology (20114ABF05100) and the Technology Plan Landing Project of Jiangxi Provincial Department of Education (GCJ2011-24).

References

(1) Zhou Y, Han S-T, Xu Z-X, Yang X-B, Ng H-P, Huang L-B, et al. Functional high-*k* nanocomposite dielectrics for flexible transistors and inverters with excellent mechanical properties. J Mater Chem. 2012;22:14246–53.
(2) Park S, Chang HY, Rahimi S, Lee AL, Tao L, Akinwande D. Transparent nanoscale polyimide gate dielectric for highly flexible electronics. Adv Electron Mater. 2018;4:1700043.
(3) Dang Z-M, Yuan J-K, Zha J-W, Zhou T, Li S-T, Hu G-H. Fundamentals, processes and applications of high-permittivity polymer–matrix composites. Prog Mater Sci. 2012;57:660–723.
(4) Zhang L, Lu X, Zhang X, Jin L, Xu Z, Cheng ZY. All-organic dielectric nanocomposites using conducting polypyrrole nanoclips as filler. Compos Sci Technol. 2018;167:285–93.
(5) Shehzad K, Ul-Haq A, Ahmad S, Mumtaz M, Hussain T, Mujahid A, et al. All-organic PANI–DBSA/PVDF dielectric composites with unique electrical properties. J Mater Sci. 2013;48:3737–44.
(6) Wang J-W, Wang Y, Wang F, Li S-Q, Xiao J, Shen Q-D. A large enhancement in dielectric properties of poly(vinylidene fluoride) based all-organic nanocomposite. Polymer. 2009;50:679–84.
(7) Zhang L, Liu Z, Lu X, Yang G, Zhang X, Cheng ZY. Nano-clip based composites with a low percolation threshold and high dielectric constant. Nano Energy. 2016;26:550–7.

(8) Yang W, Li H, Lin J, Chen G, Wang Y, Wang L, et al.. A novel all-organic DIPAB/PVDF composite film with high dielectric permittivity. J Mater Sci Mater Electron. 2017;28:9658–66.
(9) Hou H, Xu W, Ding Y. The recent progress on high-performance polymer nanofibers by electrospinning. J Jiangxi Normal Univ (Nat Sci). 2018;42:551–64.
(10) Yao K, Chen J, Li P, Duan G, Hou H. Robust strong electrospun polyimide composite nanofibers from a ternary polyamic acid blend. Compos Commun. 2019;15:92–95.
(11) Ding Y, Hou H, Zhao Y, Zhu Z, Fong H. Electrospun polyimide nanofibers and their applications. Prog Polym Sci. 2016;61:67–103.
(12) Ma P, Dai C, Wang H, Li Z, Liu H, Li W, et al. A review on high temperature resistant polyimide films: heterocyclic structures and nanocomposites. Compos Commun. 2019;16:84–93.
(13) Jiang S, Uch B, Agarwal S, Greiner A. Ultralight, thermally insulating, compressible polyimide fiber assembled sponges. ACS Appl Mater Interfaces. 2017;9:32308–15.
(14) Ma P, Dai C, Liu H. High performance polyimide films containing benzimidazole moieties for thin film solar cells. e-Polymers. 2019;19:555–62.
(15) Simpson J, Clair AS. Fundamental insight on developing low dielectric constant polyimides. Thin Solid Films. 1997;308:480–5.
(16) Chen Y, Kang E-T. New approach to nanocomposites of polyimides containing polyhedral oligomeric silsesquioxane for dielectric applications. Mater Lett. 2004;58:3716–9.
(17) Shen Y, Chen L, Jiang S, Ding Y, Xu W, Hou H. Electrospun nanofiber reinforced all-organic PVDF/PI tough composites and their dielectric permittivity. Mater Lett. 2015;160:515–7.
(18) Chisca S, Musteata VE, Sava I, Bruma M. Dielectric behavior of some aromatic polyimide films. Eur Polym J. 2011;47:1186–97.
(19) Fang D, Yao K, Ding Y, Li P, Hou H. High dielectric polyimide composite film filled with a heat-resistant organic salt. Compos Commun. 2019;14:29–33.
(20) Zhao W, Xu Y, Song C, Chen J, Liu X. Polyimide/mica hybrid films with low coefficient of thermal expansion and low dielectric constant. e-Polymers. 2019;19:181–9.
(21) Peng X, Xu W, Chen L, Ding Y, Chen S, Wang X, et al. Polyimide complexes with high dielectric performance: toward polymer film capacitor application. J Mater Chem C. 2016;4:6452–6.
(22) Yang T, Xu W, Peng X, Hou H. Crown ether-containing polyimides with high dielectric constant. RSC Adv. 2017;7:23309–12.
(23) Deligöz H, Özgümüş S, Yalçınyuva T, Yıldırım S, Değer D, Ulutaş K. A novel cross-linked polyimide film: synthesis and dielectric properties. Polymer 46:3720–9.
(24) Zhang C, Yu Y, Ding Y, Yang T, Duan G, Hou H. β-Cyclodextrin toughened polyimide composites toward all-organic dielectric materials. J Mater Sci Mater Electron. 2017;29:1182–8.
(25) Fredin LA, Li Z, Lanagan MT, Ratner MA, Marks TJ. Substantial recoverable energy storage in percolative metallic aluminum–polypropylene nanocomposites. Adv Funct Mater. 2013;23:3560–9.
(26) Chen L-H, Lin P, Ho J-C, Lee C-C, Kim C, Chen M-C. Polyimide/Ta_2O_5 nanocomposite gate insulators for enhanced organic thin-film transistor performance. Synth Met. 2011;161:1527–31.
(27) Xie S-H, Zhu B-K, Wei X-Z, Xu Z-K, Xu Y-Y. Polyimide/$BaTiO_3$ composites with controllable dielectric properties. Composites Part A. 2005;36:1152–7.
(28) Xu W, Ding Y, Jiang S, Zhu J, Ye W, Shen Y, et al. Mechanical flexible PI/MWCNTs nanocomposites with high dielectric permittivity by electrospinning. Eur Polym J. 2014;59:129–35.
(29) Lorenzini RG, Greco JA, Birge RR, Sotzing GA. Diels–Alder polysulfones as dielectric materials: computational guidance & synthesis. Polymer. 2014;55:3573–8.
(30) Labahn D, Mix R, Schönhals A. Dielectric relaxation of ultrathin films of supported polysulfone. Phys Rev E Stat Nonlinear Soft Matter Phys. 2009;79:011801.
(31) Park SJ, Kim HC. Thermal stability and toughening of epoxy resin with polysulfone resin. J Polym Sci Part B Polym Phys. 2001;39:121–8.
(32) Chen S, Hu P, Greiner A, Cheng C, Cheng H, Chen F, et al. Electrospun nanofiber belts made from high performance copolyimide. Nanotechnology. 2008;19:015604.
(33) Zhou J, Unlu M, Vega JA, Kohl PA. Anionic polysulfone ionomers and membranes containing fluorenyl groups for anionic fuel cells. J Power Sources 190:285–92.
(34) Xu W, Ding Y, Jiang S, Ye W, Liao X, Hou H. High permittivity nanocomposites fabricated from electrospun polyimide/$BaTiO_3$ hybrid nanofibers. Polym Compos. 2016;37:794–801.
(35) Wang J, Wu C, Liu R, Li S. P(VDF–TrFE–CFE)-based percolative composites exhibiting significantly enhanced dielectric properties. Polym Bull. 2013;70:1327–35.
(36) Huang C, Zhang Q. Enhanced dielectric and electromechanical responses in high dielectric constant all-polymer percolative composites. Adv Funct Mater. 2004;14:501–6.
(37) Ding Y, Wu Q, Zhao D, Ye W, Hanif M, Hou H. Flexible PI/BaTiO3 dielectric nanocomposite fabricated by combining electrospinning and electrospraying. Eur Polym J. 2013;49:2567–71.